

INFLUENCE OF ANISOTROPY ON CREEP IN A WHISKER REINFORCED MMC ROTATING DISC

S.B.SINGH*, S.RAY**, R.K.GUPTA*, AND N.S.BHATNAGAR*

*Dept. of Mathematics, **Dept. of Metallurgical and Materials Engg., University of Roorkee, Roorkee (U.P.) - 247 667

Abstract

Whisker reinforced MMC may be employed in rotating disc, a common component in friction drives, turbines and a number of other machine components, often exposed to elevated temperatures. Creep characteristics of these composites have been studied analytically using von Mises flow rule and Norton's steady state creep equations. The results for isotropic Al6061 alloy and for isotropic composite containing 20 vol% SiC_w in a matrix of Al6061 alloy have been compared with those obtained for anisotropic composites with characteristic parameters $\alpha = 0.7$ and 1.3, indicating respectively relative strengthening and weakening in the tangential direction presumably introduced by either processing or inhomogeneous distribution of reinforcement. The creep strain rates resulting in the isotropic rotating disc made of composite as well as the aluminum alloy, are tensile in the tangential direction but compressive in the axial and radial directions, also conforming to the condition of volume constancy. The creep rates in the composite are significantly reduced (by about three orders of magnitude) in all the directions compared to those observed in the base alloy. In case of anisotropy lowering the strength in the tangential direction ($\alpha > 1.0$), the radial stresses in the region near inner periphery of the disc, increase while those near the outer periphery decrease in comparison to those for the isotropic composite. But the tangential stresses reduce in the middle region of the disc and enhances near the inner and the outer periphery, when compared to those for the isotropic composite. The magnitude of stress distribution, however, changes by a small extent due to anisotropy in the disc introduced through processing or reinforcement distribution. The radial strain rate which always remained compressive for the isotropic composite and for $\alpha = 1.3$, becomes tensile in the middle region of the disc when $\alpha = 0.7$. If α is reduced from 1.3 to 0.7, the variation of tensile strain rate in the tangential direction remains similar but the magnitude reduces by five orders of magnitude. Anisotropy therefore, introduces significant change in the strain rates although its effect on the resulting stress distribution may be relatively small.

1.0 Introduction

A rotating disc at elevated temperature is a common component in aeroengines,

automobiles and in a number of other dynamic applications. A reduced weight of such components resulting from the use of aluminum base alloys in it, is expected to save power and fuel due to the increase in pay load. However, the enhanced creep of aluminum and its alloys may not permit such application. Particle and whisker reinforced metal matrix composites have shown superior high temperature properties and are finding increasing application in components exposed to higher temperature [1]. Nieh [2] has studied creep properties of Al-6061-SiC composite and his experimental results under uniaxial condition both for the composite and for the aluminum alloy show that creep is significantly reduced in the composite as compared to that in the base Al-6061 alloy. Therefore, it may be possible to employ rotating discs made of aluminum based particle or whisker reinforced composites which have isotropic mechanical properties convenient for design engineers. But, before such application, creep under the actual stress situation and under influence of anisotropy induced by processing, should be investigated to understand the long term performance of a component made of composite. The present study explores the stress distribution and the creep strain rates in the isotropic Al-6061 base alloy and the composite of the same base alloy containing 20 vol% of SiC whiskers. The influence of anisotropy has been investigated in terms of a single parameter indicating strengthening or weakening in the tangential direction in the disc introduced presumably by processing or inhomogeneous distribution of reinforcements.

2. Mathematical Formulation

2.1 Yield strengths and Hill Anisotropy Constants

When a sample disc material is tested under uniaxial loading in the r and θ direction, the corresponding stress invariant may be written in terms of the observed tensile strengths and the Hill anisotropy constants as given below.

$$\sigma_{i_1} = \sqrt{\frac{G+H}{2}} \sigma_{\theta y} \quad (1)$$

$$\sigma_{i_1} = \sqrt{\frac{F+H}{2}} \sigma_{\theta y} \quad (2)$$

When the sample is tested under uniaxial loading in the z -direction, the stress invariant may be written similarly as:

$$\sigma_{i_1} = \sqrt{\frac{F+G}{2}} \sigma_{zy} \quad (3)$$

where σ_{ry} , $\sigma_{\theta y}$ and σ_{zy} are the yield stresses in the r, θ and z directions respectively. Following Hill [3] one may write the anisotropy constants in terms of these yield stresses as

$$F = \left(\frac{1}{\sigma_{\theta y}^2} + \frac{1}{\sigma_{zy}^2} + \frac{1}{\sigma_{ry}^2} \right) \sigma_1^2 \quad (4)$$

$$G = \left(\frac{1}{\sigma_{zy}^2} + \frac{1}{\sigma_{ry}^2} + \frac{1}{\sigma_{\theta y}^2} \right) \sigma_1^2 \quad (5)$$

and

$$H = \left(\frac{1}{\sigma_{ry}^2} + \frac{1}{\sigma_{\theta y}^2} + \frac{1}{\sigma_{zy}^2} \right) \sigma_1^2 \quad (6)$$

where σ_1 is the isotropic yield stress for which $F = G = H = 1$. For simplicity one may assume that the same isotropic yield stresses are observed in the r and z directions and one may put $\sigma_{ry} = \sigma_{zy} = \sigma_1$ in Eqn. (5) and (6) to get,

$$F/H = 1 \quad (7)$$

If one assumes that a small anisotropy exists in the disc due to processing, which is reflected in the change in strength in θ direction as characterized by the ratio of their respective yield strengths, α , as given below,

$$\frac{\sigma_{ry}}{\sigma_{\theta y}} = \alpha \quad (8)$$

From Eqns. (1) and (2),

$$\alpha = \sqrt{\frac{F/H + 1}{G/H + 1}} = \sqrt{\frac{2}{G/H + 1}}$$

or

$$G/H = (2/\alpha^2) - 1 \quad (9)$$

The isotropic material corresponds to $\alpha = 1$ and the effect of a deviation of α from one on the resulting stress and creep will be investigated in the present study.

2.2 Stress and Strain Distributions in the Rotating Disc

A whisker reinforced composite disc of constant thickness and with inner and outer radii of a and b respectively, is rotating with angular velocity ω (radian/sec). From symmetry considerations, it is assumed that the principal stresses are in the radial, tangential and axial directions. For the purpose of analysis, the following further assumptions are made.

- (i) Stresses at any location of the disc remain constant in time i.e. steady state condition of stress prevails.
- (ii) Elastic deformations are small for the disc and, therefore, neglected in comparison to relatively larger creep deformation.
- (iii) Since axial stress is zero on the faces of the disc and the disc thickness is usually small compared to its diameter, the axial stress is assumed to be zero throughout the disc.
- (iv) The creep in the composite shows a steady state behavior which may be described by a power law of the form.

$$\dot{\epsilon} = B \sigma^n f(t) \quad (10)$$

where, σ is the stress and $\dot{\epsilon}$ is the strain rate under simple tension. B and n are constants of the material.

The generalized constitutive equations for creep in an anisotropic solid has been given by Gupta and Bhatnagar [4] which takes the following form when reference frame is along the principal directions of r , θ and z .

$$\begin{aligned} \dot{\epsilon}_r &= \frac{\dot{\epsilon}_i}{2\sigma_i} [(G+H) \sigma_r - H\sigma_\theta - G\sigma_z] \\ \dot{\epsilon}_\theta &= \frac{\dot{\epsilon}_i}{2\sigma_i} [(H+F) \sigma_\theta - F\sigma_z - H\sigma_r] \\ \dot{\epsilon}_z &= \frac{\dot{\epsilon}_i}{2\sigma_i} [(F+G) \sigma_z - G\sigma_r - G\sigma_\theta] \end{aligned} \quad (11)$$

where stress invariant σ_i is given by

$$\sigma_i = \frac{1}{\sqrt{2}} [F(\sigma_\theta - \sigma_z)^2 + G(\sigma_z - \sigma_r)^2 + H(\sigma_r - \sigma_\theta)^2]^{1/2} \quad (12)$$

and $\dot{\epsilon}_r$, $\dot{\epsilon}_\theta$, $\dot{\epsilon}_z$ and σ_r , σ_θ , σ_z are the strain rates and the stresses respectively in the directions indicated by subscript. $\dot{\epsilon}_i$ is the strain rate invariant, σ_i is the stress invariant and F, G, H, L, M, N are the Hill anisotropy constants of the material.

For the biaxial state of stress (σ_r , σ_θ) assumed for the rotating disc, Eqn. (12) becomes.

$$\sigma_i = \frac{1}{\sqrt{2}} [F\sigma_\theta^2 + G\sigma_r^2 + H\sigma_\theta^2]^{1/2} \quad (13)$$

and the first equation amongst the set of constitutive Eqns.(11) becomes,

$$\dot{\epsilon}_r = \frac{\dot{\epsilon}_i}{2\sigma_i} [(G+H)\sigma_r - H\sigma_\theta] \quad (14)$$

putting the value of $\dot{\epsilon}_i$ from Eqn. (10) and σ_i from Eqn. (13), one gets from Eqn. (14)

$$\frac{d\dot{u}_r}{dr} = \dot{\epsilon}_r = \frac{Bf(t)F^{(n+1)/2}}{2^{(n+1)/2}} \left[1 + \left(\frac{G}{F} + \frac{H}{F} \right) x^2 - 2 \frac{H}{F} x \right]^{(n-1)/2} \left[\left(\frac{G}{F} + \frac{H}{F} \right) x - \frac{H}{F} \right] \sigma_\theta^n \quad (15)$$

where $x = \sigma_r / \sigma_\theta$

Similarly, one may get from the second equation of Eqns. (11),

$$\frac{\dot{u}_r}{r} = \dot{\epsilon}_\theta = \frac{Bf(t)F^{(n+1)/2}}{2^{(n+1)/2}} \left[1 + \frac{H}{F} + \left(\frac{G}{F} + \frac{H}{F} \right) x^2 - 2 \frac{H}{F} x \right]^{(n-1)/2} \left[1 + \frac{H}{F} - \frac{H}{F} x \right] \sigma_\theta^n \quad (16)$$

and,

$$\dot{\epsilon}_z = -(\dot{\epsilon}_r + \dot{\epsilon}_\theta) \quad (17)$$

Dividing Eqn. (15) by Eqn. (16), one gets

$$\frac{d\dot{u}_r}{dr} \frac{r}{\dot{u}_r} = \frac{\left(\frac{G}{F} + \frac{H}{F} \right) x - \frac{H}{F}}{1 + \frac{H}{F} - \frac{H}{F} x} \quad (18)$$

Integrating Eqn. (18) between limits of a to r , one gets,

$$\dot{u}_r = \dot{u}_{r_i} \exp \left[\int_a^r \frac{\phi(r)}{r} dr \right] \quad (19)$$

where \dot{u}_{r_i} is the Radial deformation rate at internal diameter and

$$\phi(r) = \frac{\left(\frac{G}{F} + \frac{H}{F} \right) x - \frac{H}{F}}{1 + \frac{H}{F} - \frac{H}{F} x} \quad (20)$$

Dividing Eqn. (19) by r one gets $\dot{\epsilon}_\theta$ which can be equated to Eqn. (16) to get,

$$\sigma_\epsilon = \left[\frac{\dot{u}_{r_i}}{Bf(t)} \right]^{1/n} \psi(r) \quad (21)$$

where

$$\psi(r) = \left[\frac{2^{(n+1)/2} \cdot \frac{1}{r} \exp \left\{ \int_a^r \frac{\phi(r)}{r} dr \right\}}{F^{(n+1)/2} \left\{ 1 + \frac{H}{F} + \left(\frac{G}{F} + \frac{H}{F} \right) x^2 - 2 \frac{H}{F} x \right\}^{(n-1)/2} \left\{ 1 + \frac{H}{F} + \frac{H}{F} x \right\}} \right]^{1/n} \quad (22)$$

Equilibrium equation for a rotating disc of constant thickness is given by,

$$\frac{d}{dr} (r\sigma_r) - \sigma_\epsilon + \frac{\rho\omega^2 r^2}{g} = 0 \quad (23)$$

where ρ is density of the material and g is the gravitational acceleration. Integrating Eqn. (23) from a to b , and putting boundary conditions $\sigma_r = 0$ at $r = a$ and $\sigma_r = 0$ at $r = b$, one gets

$$\int_a^b \sigma_\epsilon dr = \frac{\rho\omega^2}{g} (b^3 - a^3) \quad (24)$$

From Eqns. (21) and (24) one may write,

$$\sigma_{\theta} = \left[\frac{(b-a)\sigma_{\theta_{avg}}}{\int_a^b \psi(r) dr} \right] \cdot \psi(r) \quad (25)$$

where, $\sigma_{\theta_{avg}} = \frac{1}{b-a} \int_a^b \sigma_{\theta} dr$ is the average tangential stress over the cross section.

Integrating Eqn. (23) from a to r , one may thus determine,

$$\sigma_r = \frac{1}{r} \int_a^r \sigma_{\theta} dr + \frac{\rho \omega^2}{g} \cdot \frac{(r^3 - a^3)}{r} \quad (26)$$

After finding the stresses, the strain distribution in the disc may be evaluated using Eqns. (11).

3. Numerical Calculation

The stress distribution is evaluated from the above analysis by iterative numerical scheme of computation. To find the first approximation of x , $(x)_1$ to be used in Eqns (18), (22) and (25) in the first iteration, it is assumed that $\sigma_{\theta} = \sigma_{\theta_{avg}}$ in Eqn (26) and on integration one gets first approximation of σ_r i.e. $(\sigma_r)_1$. The subscript on the first bracket has been used to indicate the number of cycle of iteration beginning with one. Then dividing $(\sigma_r)_1$ by $\sigma_{\theta_{avg}}$ one gets $(x)_1$ as given below

$$(x)_1 = \frac{(\sigma_r)_1}{\sigma_{\theta_{avg}}} = 1 - \frac{a}{r} - \frac{(r^3 - a^3)}{(b^3 - a^3)} \cdot \frac{(b-a)}{r} \quad (27)$$

Substituting this value of $(x)_1$ for x in Eqn. (18) for different values of G/F and H/F calculated as discussed in section 2, $(\phi(r))_1$ is calculated.

One carries out the numerical integration of $(\phi(r))_1$ from limits of a to r and uses this value in Eqn. (22), together with the values of G/F , H/F and $(x)_1$, to find $(\psi(r))_1$ to be used in the first iteration. Using this $(\psi(r))_1$ in Eqn. (25), $(\sigma_{\theta})_1$ is found. Using $(\sigma_{\theta})_1$ for σ_{θ} in Eqn. (26), the second approximation of σ_r i.e. $(\sigma_r)_2$ is found by numerical integration and from this the second approximation of x i.e. $(x)_2$ is found. The iteration is continued till the process converges yielding the values of stresses at different points of the radius grid. For rapid convergence 75 percent of the value of σ_{θ} obtained in the current iteration has been mixed with 25 percent of the values of σ_{θ} obtained in the last iteration for use in the next iteration. Since the problem has cylindrical symmetry the

state of stress is now completely known under condition of creep. The strain rates are calculated now from the Eqns. (15), (16) and (17) which are derived from the constitutive Eqns. (11). Integrating these equations of strain rates to a given time one gets the strain in the disc in different points of the grid after a given period of time which is 180 hours for the present case.

Creep constants B and n used in Eqn. (10) have been taken from the study of Nieh[2] for 6061 Al and 6061 Al-20 wt % SiC whisker composite. Steady state creep law for the composite has been given as

$$\dot{\epsilon}_{ss} = 1.5 \times 10^{-9} \sigma^{20.5} \exp\left(\frac{-Q_a}{RT}\right) \quad (28)$$

Where ϵ_{ss} is the steady state creep rate in sec^{-1} , σ is the applied stress in units of MPa, $Q_a = 390$ kJ/mole is the apparent activation energy, T is the temperature in K and R is the universal gas constant. Based on the experimental results of Nieh[2], the creep law for 6061 Al alloy has been taken as

$$\dot{\epsilon}_{ss} = 8.99 \times 10^{-14} \sigma^{4.19} \quad (29)$$

The results obtained from the scheme of computation as described above for isotropic alloy and whisker reinforced composite have been compared with those composites which have developed a degree of anisotropy. These results are discussed in the next section.

4. Discussion

The variations of radial stresses and tangential stresses in the isotropic discs made of 6061 aluminum alloy and Al-20v% SiC composites respectively rotating at 15,000 rpm and undergoing steady state creep at 516 K, are shown in Figs. 1 and 2. It is observed that the radial stresses are more in the case of aluminum alloy than those in the composite and in both these cases the radial stress reduces to zero in the free radial boundary at $r = a$ and $r = b$ as imposed. It is interesting to observe that in the case of aluminum alloy the stresses are more inspite of the composite having about 2% higher density. This situation may be clearly understood from Eqn.(26) which expresses radial stress in terms of an integral over tangential stress and a negative second term which has a higher value at higher density. The dominance of the density dependent term may have resulted in a lower radial stress in the composite compared to that in the aluminium alloy. The relative importance of the term involving the integral over the tangential stress may be assessed from Fig.2 which shows that at lower radial distances, the tangential stresses in the aluminium alloy are more than that in the composite. However, towards the outer periphery, the tangential stresses in the composite are

more than those in the aluminium alloy. It is also interesting to note that tangential stresses in the aluminum alloy are monotonically decreasing towards the outer periphery but those in the composite has a maximum. It should also be noted that the maximum tangential stress is about twice as large as the maximum radial stress.

The variation of tangential stress depends on the ratio of the value of $\psi(r)$ at a given radial distance to its average value, multiplied by the average value of σ_{θ} which is dependent on density, as shown in Eqns. (24) and (25). The average value of σ_{θ} does not depend on radial distance and so the variation of tangential stress will reflect only variation of $\psi(r)$. Fig.3 shows the variation of $\psi(r)$ which is dependent on the stress exponent, n , in Norton equation as shown in Eqn. (22). It is observed that the composite has a higher $\psi(r)$ as compared to that in the aluminium alloy. Further, $\psi(r)$ is monotonic in the case of aluminium alloy but in case of composite it has a maximum. In case of composite, a higher average value of σ_{θ} could not result in a higher value of tangential stress at lower radial distance because in this region the value of $\psi(r)$ is lower than that of its average value. But in the case of aluminum alloy the value of $\psi(r)$ at lower radial distances is larger than its average value. Therefore, the aluminium alloy has a relatively larger tangential stress at lower radial distances. The relative values of $\psi(r)$ and its average changes in the composite and the aluminium alloy resulting in changes in tangential stresses are shown in Fig.2.

The variations of radial strain rate which is compressive in the isotropic discs made of both 6061 aluminium alloy and Al-20 vol% SiC composite are shown in Fig.4. It is observed that the radial strain rate in the composite is about three orders of magnitude lower than the strain rate in the aluminium alloy. Also it is observed that the radial strain rate in the middle of the disc is less in comparison to those at the inner or outer periphery. This is due to the variation in the values of the expression in the square brackets in Eqn.(15) taken together, involving the anisotropy constants ($F=G=H=1$ for isotropic case) and x , the ratio of radial to tangential stress. The variation in tangential stress is not able to dominate the trend in radial strain rate. The values of these expressions in square brackets in Eqn.(15) taken together, are unity at the inner and outer periphery of the disc and lower in the middle and the radial strain rate following the same trend.

Fig.5 shows the tangential strain rate in the isotropic discs made of both 6061 aluminium alloy and Al-20 vol% SiC composite. It is observed that the tangential strain rates are tensile at all points in a isotropic disc. But it is not following the trends of variation of tangential stress but the one dictated by the expressions in the square brackets in Eqn.(16) taken together and it depends on the Hill anisotropy constants ($F=G=H=1$ for isotropic case) and the ratio of radial to tangential stress. The variation of compressive axial strain rates in the discs made of both 6061 aluminium alloy and Al-20 vol% SiC composite are shown in Fig.6.

The variation of stresses and strain rates in an anisotropic disc characterized by parameter α deviating from unity, have been investigated and the results in respect of difference of radial and tangential stresses over those in isotropic case are shown in Figs. 7 and 8 respectively. Since it has been assumed that $F/H = 1$ even for the anisotropic case, α less than or greater than unity will imply respectively strengthening or weakening in the tangential direction. If α is less than unity the radial stresses in the region near inner periphery of the disc increase while those near the outer periphery decrease with respect to that in isotropic case. For the same value of α the tangential stresses reduce in the middle region of the disc in comparison to that in isotropic case but enhances near the inner and the outer periphery as shown in Fig. 8. These trends of variation for the radial and tangential stresses are reversed when α is greater than unity. However, the magnitude of this change is only a few percent. Therefore, it is evident that the stress distribution may not change significantly due to anisotropy introduced by processing or inhomogeneous distribution of reinforcement.

It is clear from the Eqns. (16), (17) and (18) that the strain rates in directions r , θ , z are very much dependent on the value of x , $\phi(r)$ and $\psi(r)$. The values of x i.e., the ratio of radial to tangential stresses, have been plotted against radius in Fig. 9 for different values of α . Near the inner periphery, x is very nearly the same but the values start to differ towards the middle of the disc particularly if α is lower than unity. Beyond the midpoint of the disc the values of x differ and larger α results in larger values of x as shown in Fig. 9. However, the magnitude of change in x with α is quite small. The most interesting change with anisotropy is observed in the $\phi(r)$ as shown in Fig. 10. When α is larger than unity, $\phi(r)$ remains negative as in the isotropic case and the trend of variation is also similar to that of isotropic case where there is one maximum in the middle. But when α is lower than unity, $\phi(r)$ is negative near the inner and the outer periphery, but it becomes positive in the middle of the disc. The trend of variation of $\phi(r)$ also changes from one maximum for $\alpha \geq 1.0$ to two maximas in the middle region for $\alpha < 1.0$. These changes in $\phi(r)$ are due to increase in values of G/F because of lower α making the numerator of Eqn. (20) positive for certain values of x . The variation of $\psi(r)$ with radius for different α is shown in Fig. 11 and the values are all positive. When α is higher than unity, there is one maximum in $\psi(r)$ in the middle of the disc and the trend variation remains similar to that observed in the isotropic case. When α is less than unity, the trend of variation of $\psi(r)$ is, changed from that for the isotropic case to one with two maximum.

Fig. 12, 13 and 14 show respectively the radial, the tangential and the axial strain rates in the different locations in the disc. It is observed in Fig. 12(a) and (c) that the radial strain rate which always remained compressive for the isotropic case and the case where α is greater than unity, becomes tensile in the middle region of the disc when α is less than unity. This is the consequence of the change in sign of

$$\left[\left(\frac{G}{F} + \frac{H}{F} \right) x - \frac{H}{F} \right] \text{ in } \phi(r) \text{ as shown in Fig. 10 and this is responsible for the resulting}$$
 tensile radial strain rate given by Eqn.(15). This distribution of strain due to the anisotropy in the disc, may cause unwanted deformation in shape. It is, however, interesting that the trend of variation of tensile strain rate in the tangential direction remains the same although the magnitude reduces by five orders of magnitude as shown in Fig. 13, if α is reduced from 1.3 to 0.7 i.e., the strength in the tangential direction is enhanced. The axial strain rate in Fig. 14 conforms to the constraint of material conservation and so, its trend of variation has been decided by the trend of variation in radial strain rate as the trend of variation of tangential strain rate does not change in the range of anisotropy investigated here. For $\alpha=0.7$ the axial strain rate in Fig. 14 shows a compensating change in the trend compatible to the change in radial strain rate for this case as shown in Fig. 12.

5. Conclusions

The study reported in this paper has lead to following conclusions ;

- (1) In the rotating disc made of isotropic composite containing 20 vol% of silicon carbide whisker in base 6061 aluminum alloy, the tensile stress developing in the tangential direction and the compressive stress developing in the radial direction are lower in magnitude than those in the disc made of base alloy.
- (2) The creep strain rates resulting in the isotropic rotating disc made of composite as well as the aluminum alloy, are tensile in the tangential direction but compressive in the axial and the radial directions, also conforming to the condition of volume constancy. The creep rates in the composite are significantly reduced in all the directions compared to those observed in the base alloy.
- (3) In case of anisotropy lowering the strength in the tangential direction ($\alpha > 1.0$), the radial stresses in the region near inner periphery of the disc increase while those near the outer periphery decrease in comparison to those for the isotropic composite. But the tangential stresses reduce in the middle region of the disc and enhances near the inner and the outer periphery, when compared to those for the isotropic composite. The magnitude of stress distribution, however, changes by a small extent due to anisotropy in the disc introduced through processing or reinforcement distribution.

- (4) When α is greater than unity, the trends of variation for the radial stresses and tangential stresses are reverse of those found for $\alpha > 1.0$ but the change in magnitude of stresses is relatively small.
- (5) The radial strain rate is compressive when α is greater than unity ($\alpha = 1.3$), similar to that for the isotropic composites. The tangential creep rate is also tensile and reduces by about three orders of magnitude compared to those for isotropic composite.
- (6) The radial strain rate which always remained compressive for the isotropic composite and for $\alpha > 1.0$, becomes tensile in the middle region of the disc when α is less than unity ($\alpha = 0.7$). If α is reduced from 1.3 to 0.7, the trend of variation of tensile strain rate in the tangential direction remains the same although the magnitude reduces by about five orders of magnitude. The axial strain rate conforms to the constraint of material conservation.
- (7) Anisotropy introduces significant change in the strain rates and if strength in tangential direction is enhanced, it may cause unwanted deformations in shape but its effect on the resulting stress distribution may be relatively small.

References

1. P.K.Ghosh and S.Ray; *J.Mat.Sc.*, **22** (1987) 4077-4081.
2. T.G.Nieh; *Met. Trans. A*, **15A** (1982) 139-145.
3. R.Hill; *The Mathematical Theory of Plasticity*, Oxford University Press London, 1950.
4. R.P.Gupta and N.S.Bhatnagar; *Wood Science and Technology*, **1** (1967) 142-148.

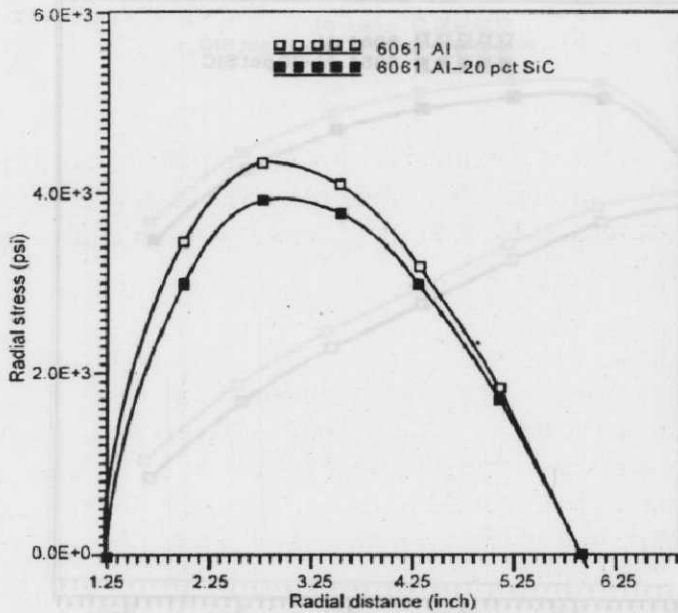


Fig. 1 - Variation of radial stress in an isotropic disc rotating with an angular velocity of 15000 rpm at 516 K

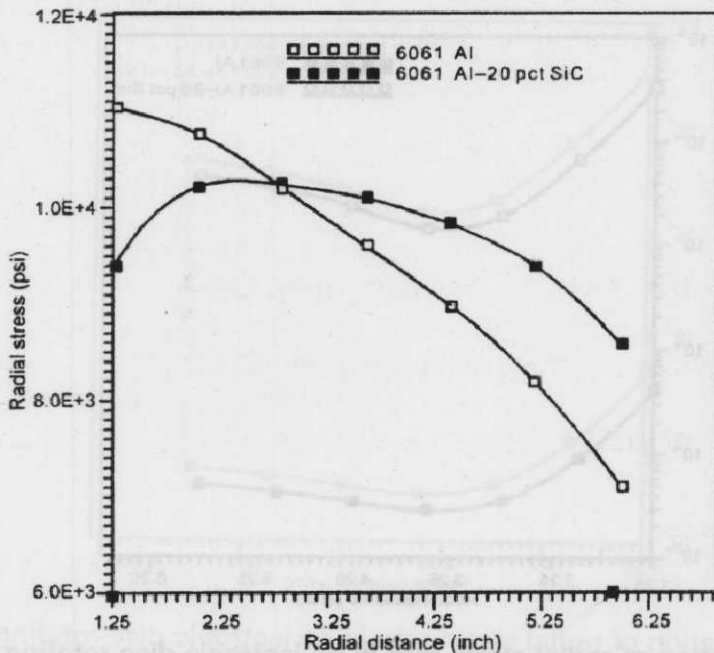


Fig. 2 - Variation of tangential stress in an isotropic disc rotating with an angular velocity of 15000 rpm at 516 K

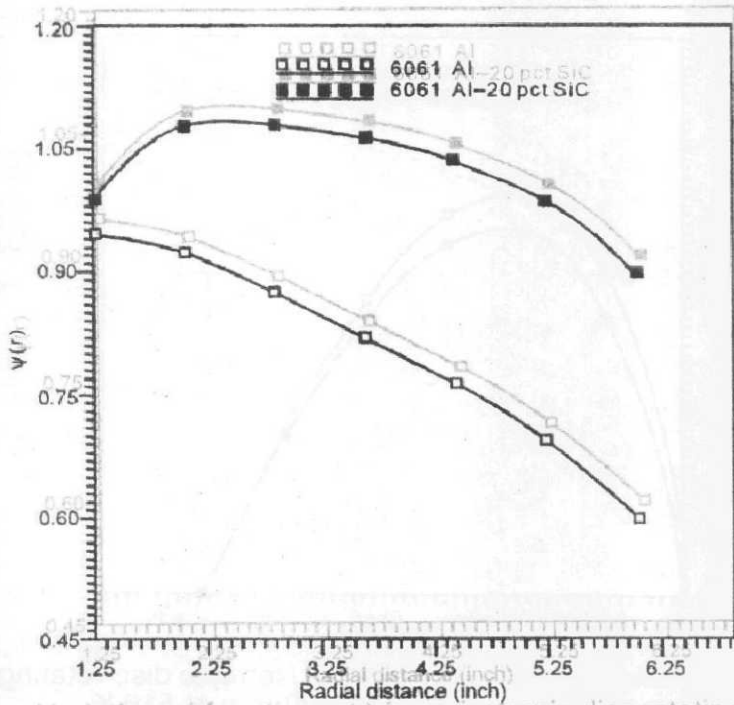


Fig. 3 - Variation of function $\psi(r)$ in an isotropic disc rotating with an angular velocity of 15000 rpm at 516 K

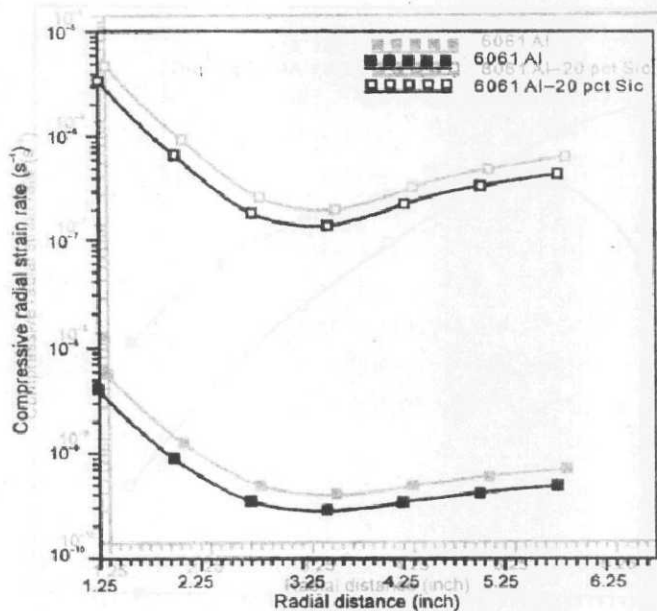


Fig. 4 - Variation of radial strain rate in an isotropic disc rotating with an angular velocity of 15000 rpm at 516 K

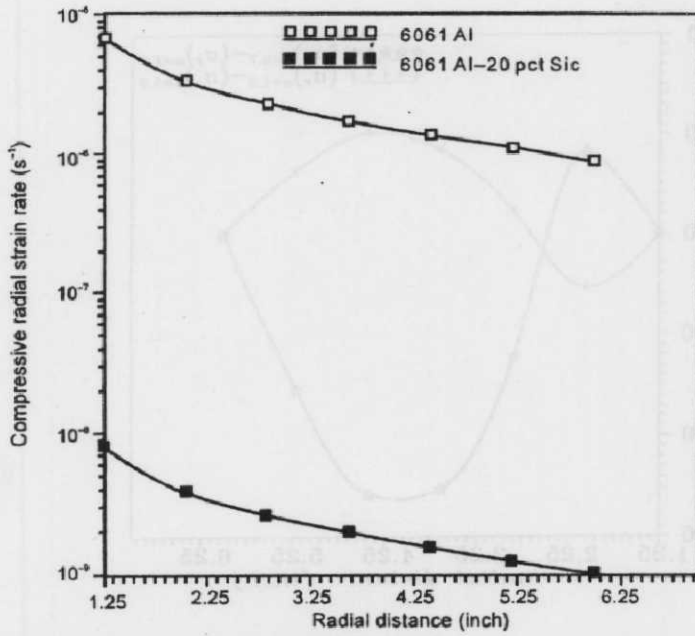


Fig. 5 - Variation of tangential strain rate in an isotropic disc rotating with an angular velocity of 15000 rpm at 516 K

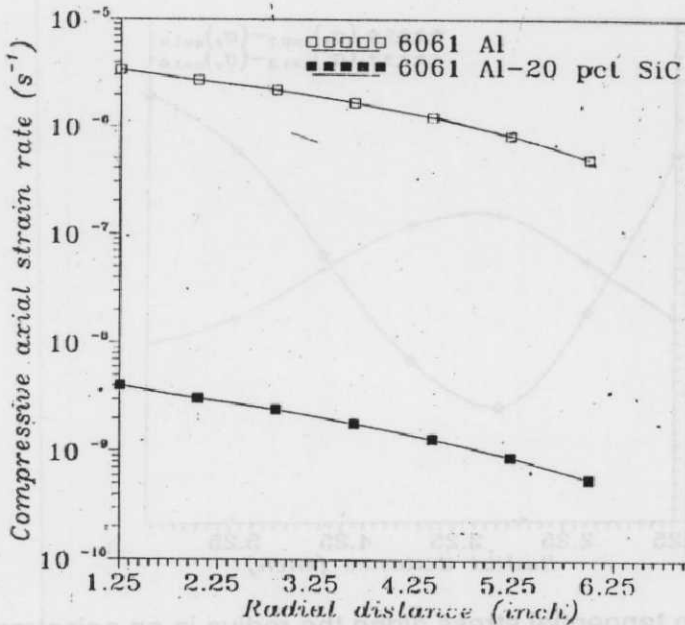


Fig. 6 - Variation of axial strain rate in an isotropic disc rotating with an angular velocity of 15000 rpm at 516 K

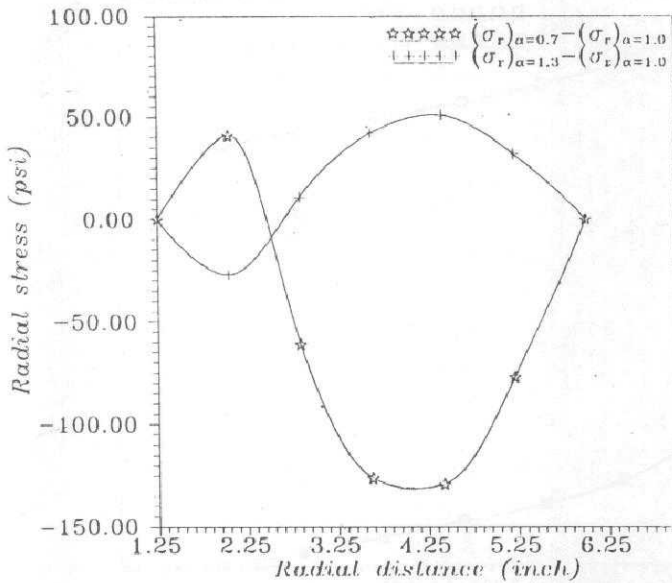


Fig. 7 - Change in radial stress along the radius in an anisotropic disc ($\alpha = 0.7$ & 1.3) over that in an isotropic disc ($\alpha = 1.0$), both rotating with an angular velocity of 15000 rpm at 516 K.

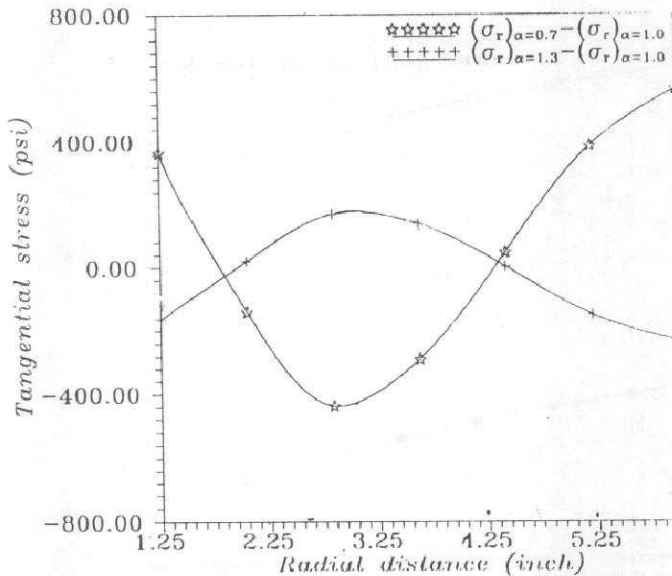


Fig. 8 - Change in tangential stress along the radius in an anisotropic disc ($\alpha = 0.7$ & 1.3) over that in an isotropic disc ($\alpha = 1.0$), both rotating with an angular velocity of 15000 rpm at 516 K.

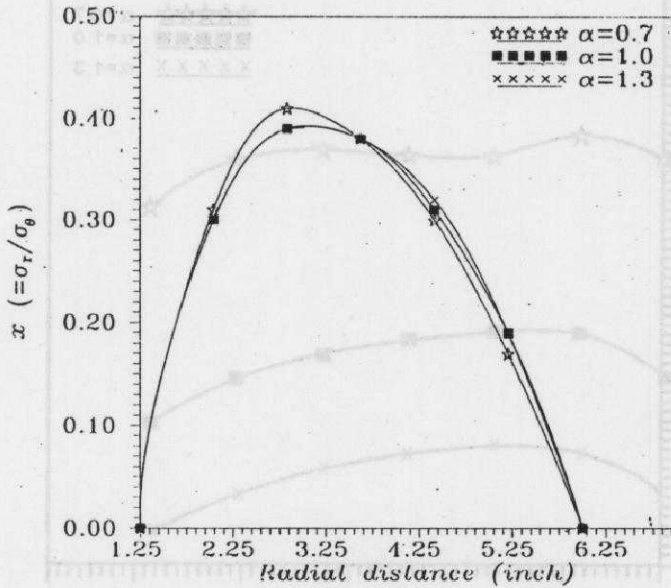


Fig. 9 - Variation of $x = (\sigma_r/\sigma_\theta)$ along the radius in both isotropic ($\alpha = 1.0$) & anisotropic ($\alpha = 0.7$ & 1.3) discs rotating with an angular velocity of 15000 rpm at 516K

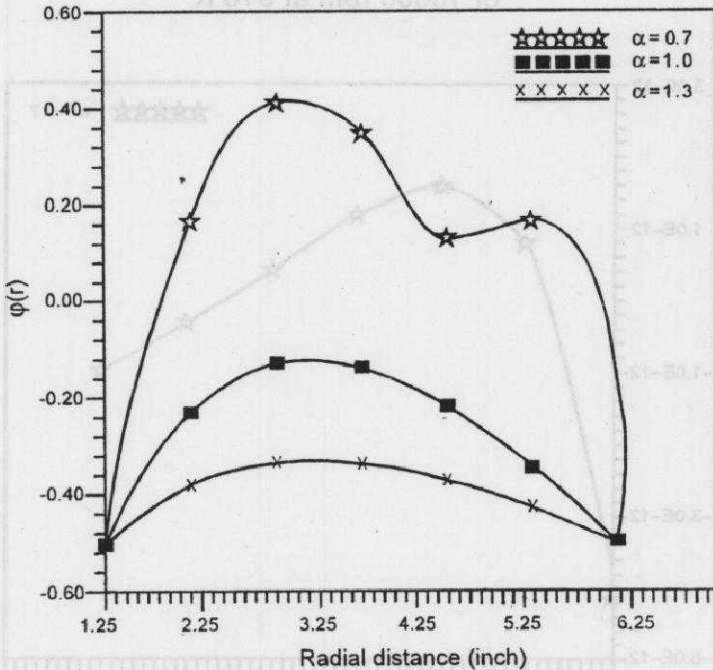


Fig. 10 - Variation of function $\phi(r)$ along the radius in both isotropic ($\alpha = 1.0$) & anisotropic ($\alpha = 0.7$ & 1.3) discs rotating with an angular velocity of 15000 rpm at 516K

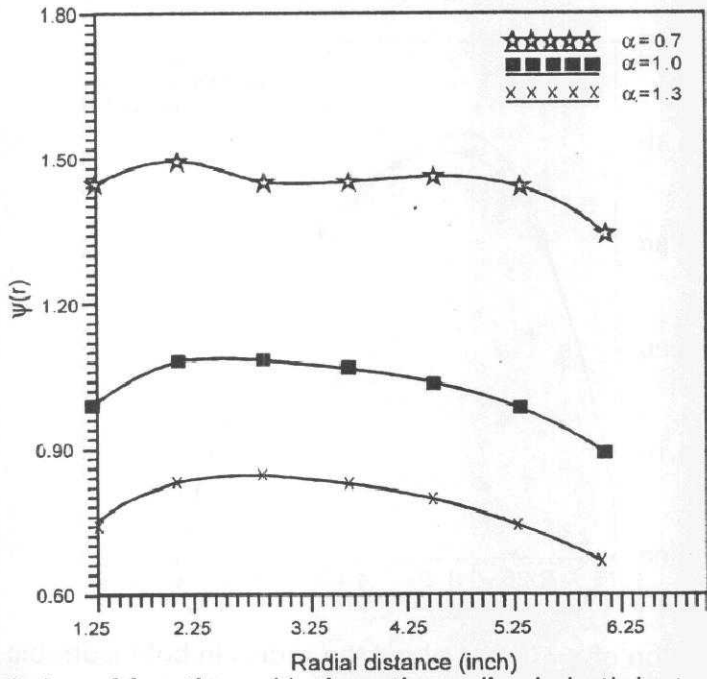


Fig. 11 - Variation of function $\psi(r)$ along the radius in both isotropic ($\alpha = 1.0$) & anisotropic ($\alpha = 0.7$ & 1.3) discs rotating with an angular velocity of 15000 rpm at 516 K

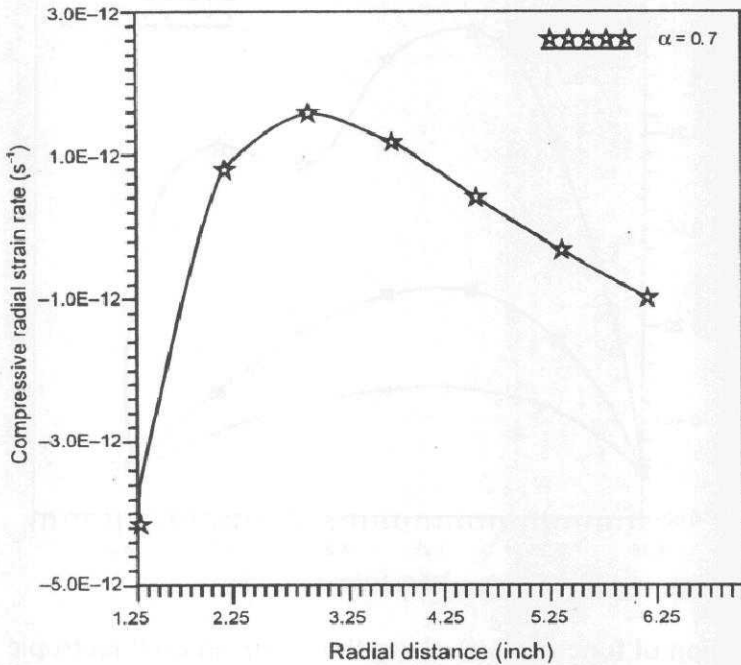


Fig. 12(a) - Variation of radial strain rate in an anisotropic ($\alpha = 0.7$) discs rotating with an angular velocity at 15000 rpm at 516 K

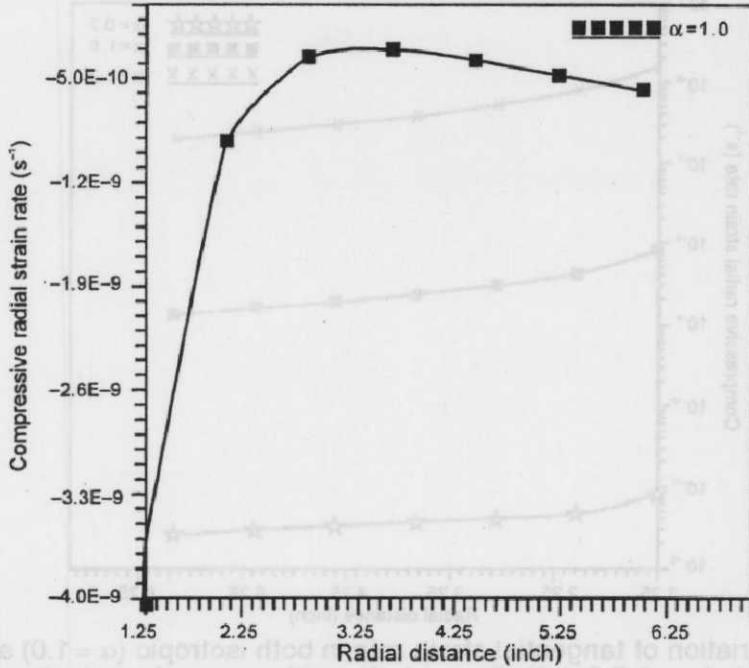


Fig. 12(b) - Variation of radial strain rate in an anisotropic ($\alpha = 1.0$) discs rotating with an angular velocity at 15000 rpm at 516 K

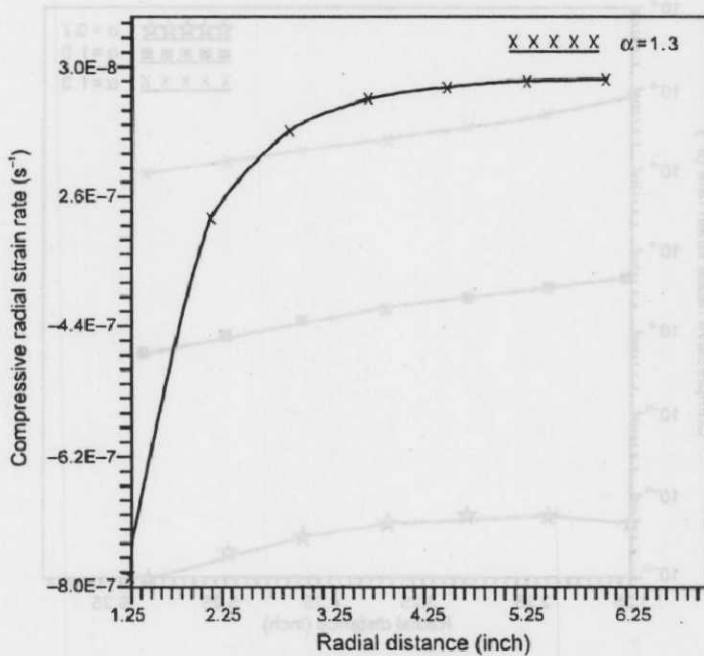


Fig. 12(c) - Variation of radial strain rate in an anisotropic ($\alpha = 1.3$) disc rotating with an angular velocity of 15000 rpm at 516 K

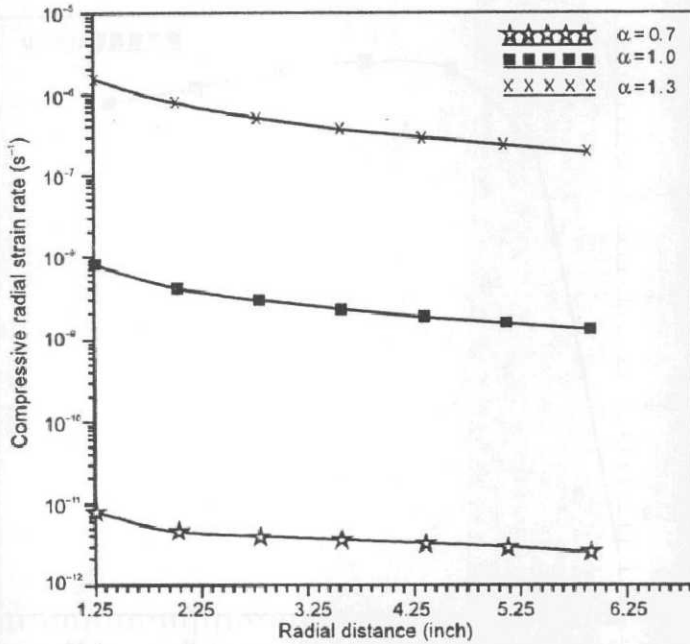


Fig. 13 - Variation of tangential strain rate in both isotropic ($\alpha = 1.0$) and anisotropic ($\alpha = 0.7$ & 1.3) discs rotating with an angular velocity of 15000 rpm at 516 K

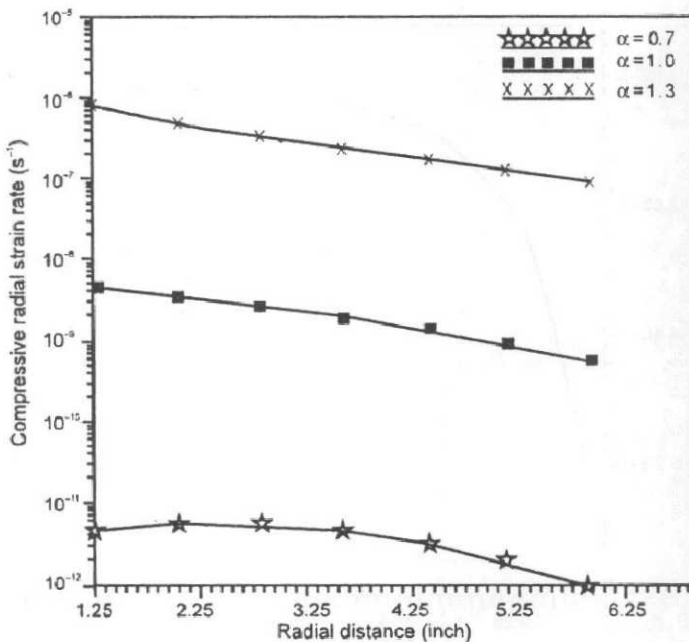


Fig. 14 - Variation of axial strain rate in both isotropic disc ($\alpha = 1.0$) and anisotropic ($\alpha = 0.7$ & 1.3) disc rotating with an angular velocity of 15000 rpm at 516 K